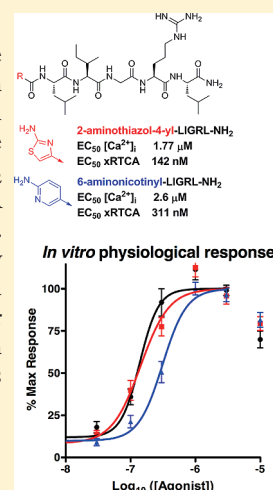


Potent Agonists of the Protease Activated Receptor 2 (PAR<sub>2</sub>)Scott Boitano,<sup>†,‡</sup> Andrea N. Flynn,<sup>†,‡</sup> Stephanie M. Schulz,<sup>†,‡</sup> Justin Hoffman,<sup>†,‡</sup> Theodore J. Price,<sup>§</sup> and Josef Vagner<sup>\*,‡</sup><sup>†</sup>Arizona Respiratory Center and Department of Physiology, University of Arizona, 1501 N. Campbell Avenue, Tucson, Arizona 85724, United States<sup>‡</sup>The BIO5 Research Institute, University of Arizona, 1657 E. Helen Street, Tucson, Arizona 85721, United States<sup>§</sup>Department of Pharmacology, University of Arizona, 1501 N. Campbell Avenue, Tucson, Arizona 85724, United States

## Supporting Information

**ABSTRACT:** Novel peptidomimetic pharmacophores to PAR<sub>2</sub> were designed based on the known activating peptide SLIGRL-NH<sub>2</sub>. A set of 15 analogues was evaluated with a model cell line (16HBE14o-) that highly expresses PAR<sub>2</sub>. Cells exposed to the PAR<sub>2</sub> activating peptide with N-terminal 2-furoyl modification (2-furoyl-LIGRLO-NH<sub>2</sub>) initiated increases in intracellular calcium concentration ([Ca<sup>2+</sup>]<sub>i</sub>; EC<sub>50</sub> = 0.84 μM) and in vitro physiological responses as measured by the xCELLigence real time cell analyzer (RTCA EC<sub>50</sub> = 138 nM). We discovered two selective PAR<sub>2</sub> agonists with comparable potency: compound 1 (2-aminothiazol-4-yl; Ca<sup>2+</sup> EC<sub>50</sub> = 1.77 μM, RTCA EC<sub>50</sub> = 142 nM) and compound 2 (6-aminonicotinyl; Ca<sup>2+</sup> EC<sub>50</sub> = 2.60 μM, RTCA EC<sub>50</sub> = 311 nM). Unlike the previously described agonist, these novel agonists are devoid of the metabolically unstable 2-furoyl modification and thus provide potential advantages for PAR<sub>2</sub> peptide design for in vitro and in vivo studies. The novel compounds described herein also serve as a starting point for structure–activity relationship (SAR) design and are, for the first time, evaluated via a unique high throughput in vitro physiological assay. Together these will lead to discovery of more potent agonists and antagonists of PAR<sub>2</sub>.



## INTRODUCTION

Protease-activated receptors (PARs) 1–4 are a family of four G-protein-coupled receptors (GPCRs) that are self-activated by a tethered sequence exposed by proteolysis of the extracellular domain.<sup>1</sup> The four members of the GPCR family of PARs are expressed on a wide variety of cell types. PARs are activated by proteolysis in response to endogenous and exogenous proteases and can contribute to both cellular homeostasis and pathology.<sup>1,2</sup> In the case of PAR<sub>2</sub>, the exposed peptides such as SLIGVK-NH<sub>2</sub> (human) or SLIGRL-NH<sub>2</sub> (murine) remain tethered on the receptor and activate an orthosteric binding site located on second loop of the receptor.<sup>1</sup> The different N-termini of the PARs present substrates for a variety of proteases that create selective activation mechanisms for signal transduction. This enzyme-linked self-activation is limited to PARs among GPCRs.<sup>3</sup> There are a variety of enzymes that can expose the tethered ligand on PAR, but a key difference between PAR<sub>2</sub> and the other PARs is the lack of activation by thrombin.<sup>4</sup> As an obvious consequence of its activation mechanism, PAR<sub>2</sub> is associated with pathologies with a strong protease release. The involvement of PAR<sub>2</sub> in inflammatory diseases such as arthritis, lung inflammation (asthma), inflammatory bowel disease, sepsis, and pain disorders makes PAR<sub>2</sub> an attractive target for drug intervention.

Significant tools used to study PARs are small peptides or peptidomimetics that mimic the ligand binding properties of the tethered ligand exposed by proteolysis of the N-terminus from the natural receptor (reviewed in ref 1b): SFLLRN-NH<sub>2</sub> activates PAR<sub>1</sub>; human-derived SLIGKV-NH<sub>2</sub> and murine-derived SLIGRL-NH<sub>2</sub> activate PAR<sub>2</sub>; GYPQVN-NH<sub>2</sub> activates PAR<sub>4</sub>. However, these short peptides activate cognate receptors with lower potency compared with native tethered ligands, which require lower binding energy as a consequence of the covalent link to the receptor. Also, untethered activating peptides have the potential to react across PARs. For example, the PAR<sub>1</sub> activating peptide SFLLRN-NH<sub>2</sub> can also activate PAR<sub>2</sub>.<sup>5</sup> In lieu of this caveat, activating peptides/peptidomimetics provide useful tools for establishment of SAR and rational drug design because they limit off-target effects that are often a complication of natural protease activation and allow for a more potent and specific activation of individual PARs. Indeed, the most potent PAR<sub>2</sub> agonist reported to date was developed by modifying a known activating peptide sequence.<sup>6</sup> The N-terminal serine of SLIGRL-NH<sub>2</sub> was substituted with 2-furoyl, and the resulting analogue

Received: October 11, 2010

Published: February 04, 2011

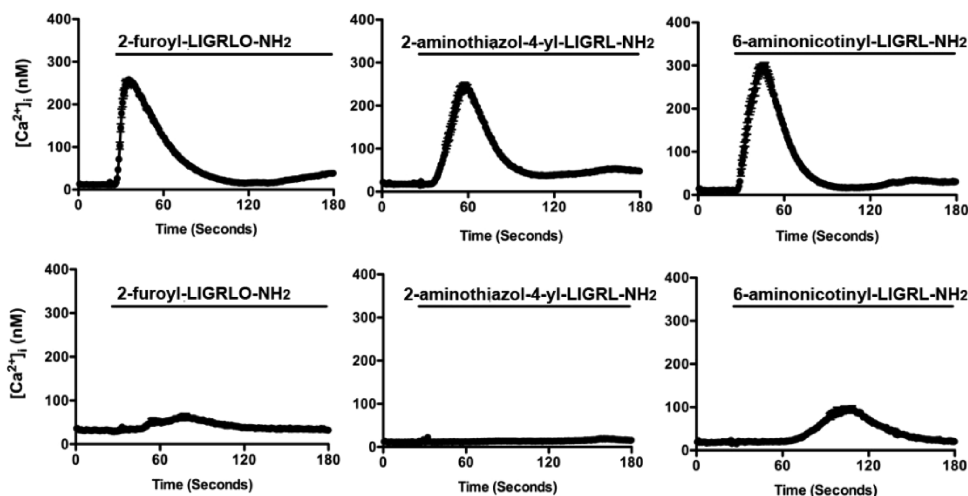


**Figure 1.**  $\text{Ca}^{2+}$  signaling induced by novel agonists in the presence or absence of  $\text{PAR}_2$ : typical experiments showing the average  $[\text{Ca}^{2+}]_i$  ( $\pm$ SEM) plotted over time for all cells ( $\sim 90$ ) in a single experiment following agonist exposure. In each experiment  $5 \mu\text{M}$  agonist was added (denoted by line) to  $\text{PAR}_2$  expressing kNRK cells (top) or plasmid expressing control kNRK cells (bottom). In the  $\text{PAR}_2$ -transfected cells, agonists induce rapid and robust changes in  $[\text{Ca}^{2+}]_i$ . However, in the absence of  $\text{PAR}_2$  overexpression,  $[\text{Ca}^{2+}]_i$  response is minimal. Similar traces are observed with  $\text{PAR}_2$ -transfected/nontransfected HeLa cells (not shown).

2-furoyl-LIGRLO-NH<sub>2</sub> is 10–25 times more efficient at increasing  $[\text{Ca}^{2+}]_i$  in human and rat  $\text{PAR}_2$  expressing cells.<sup>6,7</sup> The development of 2-furoyl-LIGRLO-NH<sub>2</sub> significantly moved research toward a better understanding of  $\text{PAR}_2$  agonist activity and established a platform for rational peptidomimetic design. Such peptides, peptidomimetics, and other small molecules<sup>8</sup> have been demonstrated to have increased specificity and affinity for  $\text{PAR}_2$  and have been used to both activate  $\text{PAR}_2$  and, in high concentrations, desensitize cells to subsequent  $\text{PAR}_2$  responses in model cells.<sup>6,7,9</sup> Besides therapeutic intervention, agonists of  $\text{PAR}_2$  can serve as tools for SAR and for defining the cellular and molecular signaling mechanisms that may contribute to pathology.

Although 2-furoyl-LIGRLO-NH<sub>2</sub> has been useful in many  $\text{PAR}_2$  cellular and molecular studies, the furane ring is not considered as a safe structural element for drug design.<sup>10</sup> Furane-containing drugs (including the structurally similar 2-acetyl furane and at least eight other drugs like the diuretic drug furosemide) can be metabolically activated by cytochrome P450 to form electrophilic intermediates ( $\gamma$ -ketocarboxylic acids) by oxidative opening of the furane heterocycle. These reactive metabolites have been shown to bind covalently to liver proteins and cause hepatotoxicity in vivo. Because furane-based structures present a potential risk for hepatotoxicity, substitutes for the furane in 2-furoyl-LIGRLO-NH<sub>2</sub> may provide a more optimal drug design paradigm.

Despite the potential for drug development from known peptide/peptidomimetic  $\text{PAR}_2$  agonists as starting points for drug discovery (e.g., SLIGVK-NH<sub>2</sub>, SLIGRL-NH<sub>2</sub> and 2-furoyl-LIGRLO-NH<sub>2</sub>), there are limited reports on SAR<sup>5,8b,11</sup> and a limited selection of small molecule compounds that can be used as tools to understand the contribution of  $\text{PAR}_2$  to cellular and tissue function. We hypothesized that the 2-furoyl residue could be substituted by other metabolically stable heterocycles at the N-terminus of the peptide. Consistent with this hypothesis, Barry et al.<sup>8b</sup> has presented a small compound library based on a X-LIGRLI-NH<sub>2</sub> hexapeptide motif. Results using a  $\text{Ca}^{2+}$  mobilization cellular assay to evaluate the X-LIGRLI-NH<sub>2</sub> library showed that (i) no heterocyclic substitution was better than 2-furoyl-LIGRLI-NH<sub>2</sub>, (ii) aliphatic residues lead to less  $\text{Ca}^{2+}$  mobilization,

(iii) aromatic residues were required, but electron donating effects of the heteroatom can potentiate the activity (2-furoyl-LIGRLI-NH<sub>2</sub>,  $\text{EC}_{50} = 0.16 \mu\text{M}$ , compared to 4-phenyl-LIGRLI-NH<sub>2</sub>,  $\text{EC}_{50} = 0.8 \mu\text{M}$ , and (iv) steric effects can diminish activity (2-furoyl-LIGRLI-NH<sub>2</sub>,  $\text{EC}_{50} = 0.16 \mu\text{M}$ , compared to 2-benzofuranyl-LIGRLI-NH<sub>2</sub>,  $\text{EC}_{50} = 0.25 \mu\text{M}$ ; phenyl-LIGRLI-NH<sub>2</sub>,  $\text{EC}_{50} = 0.8 \mu\text{M}$ , compared to 4-biphenyl-LIGRLI-NH<sub>2</sub>,  $\text{EC}_{50} = 15.8 \mu\text{M}$ ). These results supported our hypothesis that a metabolically stable modification of 2-furoyl-LIGRLO-NH<sub>2</sub> can be found. We focused our initial design on truncation and conformational constraint of the peptide chain in an effort to move toward small molecule drug design for  $\text{PAR}_2$ . Here, we present potential  $\text{PAR}_2$  ligands based on the shortened pentapeptide sequence X-LIGRL-NH<sub>2</sub>.

## RESULTS

**Synthesis.** Compound peptidomimetics were synthesized using standard Fmoc chemistry on Rink amide resin.<sup>12</sup> Compounds were cleaved off the resin with TFA-scavenger cocktails and purified by PR-HPLC and/or size-exclusion chromatography. All compounds were 95%+ pure from analytical HPLC and expected MS results.

**Agonist Design.** Our goal was to design potent and selective agonists of  $\text{PAR}_2$  that contain a metabolically stable substitution of the furane ring at the N-terminus. Furthermore, we strived to modify the peptide portion of the agonist into a peptidomimetic structure to increase stability for systemic applications. In contrast to a previous reported library used to help guide our design,<sup>8b</sup> we used the LIGRL-NH<sub>2</sub> pentapeptide instead of the more active but longer heptapeptides X-LIGRL-NH<sub>2</sub>.

**$\text{Ca}^{2+}$  Mobilization Assay.** A set of 15 compounds based on the X-LIGRL-NH<sub>2</sub> sequence were first screened in model epithelial cells (16HBE14o-) by monitoring changes in  $[\text{Ca}^{2+}]_i$  in response to an initial compound dose of  $100 \mu\text{M}$  (based on activity of native SLIGRL-NH<sub>2</sub> peptide activation).  $[\text{Ca}^{2+}]_i$  was determined for 80–100 cells using the  $\text{Ca}^{2+}$ -sensitive fluorescent dye fura-2 and digital imaging microscopy.<sup>13</sup> To quantify the response, cells were determined to be “activated” if their

Table 1. Ca<sup>2+</sup> Mobilization and in Vitro Physiological (RTCA) Assays

R-CO-Leu-Ile-Gly-Arg-Leu-NH <sub>2</sub> <sup>a</sup>	[Ca <sup>2+</sup> ] <sub>i</sub> measurements				xRTCA <sup>b</sup> EC <sub>50</sub> (nM)
	% response 100 μM	% response 10 μM	% response 2.5 μM	EC <sub>50</sub> (μM)	
2-furoyl-Leu-Ile-Gly-Arg-Leu-Orn(Aloc)-NH <sub>2</sub>	100 ± 0	97.8 ± 1.0	93.6 ± 3.3	0.84 ± 0.08	138 ± 13
1 2-aminothiazol-4-yl	100 ± 0	96.2 ± 1.4	67.5 ± 7.5	1.77 ± 0.24	142 ± 18
2 6-aminonicotinyl	100 ± 0	93 ± 2.0	55 ± 11.6	2.60 ± 0.32	311 ± 26
3 6-aminopyridin-2-yl	99.3 ± 0.7	94.4 ± 2.6	27.1 ± 6.9	3.50 ± 0.36	ND
4 4-aminophenyl	93.0 ± 0.3	86.9 ± 4.1	16.5 ± 5.3	6.59 ± 1.7	ND

<sup>a</sup>The structures do not contain C-terminal Orn as 2-furoyl-Leu-Ile-Gly-Arg-Leu-Orn(Aloc)-NH<sub>2</sub>. <sup>b</sup>EC<sub>50</sub> = concentration of compound that was able to generate 50% maximal intracellular activity. Values are expressed ± SEM ( $N \geq 2$  for 100 μM;  $N \geq 4$  for all others in Ca<sup>2+</sup> assay; data are expressed % response ± SEM;  $N \geq 8$  in the RTCA assay). ND = not determined.

[Ca<sup>2+</sup>]<sub>i</sub> reached 200 nM or more (from a resting value of 50–75 nM) in a 3 min time period. The percentage of activated cells for each experiment was determined. Compounds 11–16 lacked activity in the Ca<sup>2+</sup> mobilization assay (0% activated cells) at 100 μM dose and were eliminated from further screening. Compounds 5–10 activated cells at doses of 100 μM but failed to activate cells at doses of 2.5 μM (for details see Supporting Information Table S1). Compounds 1–4 displayed activated Ca<sup>2+</sup> responses in a significant percentage of cells (>5%) at doses of ≤2.5 μM. EC<sub>50</sub> values were calculated for these four agonists. As a point of reference, SLIGRL-NH<sub>2</sub> has an approximate EC<sub>50</sub> of >40 μM in this assay (data not shown).

Because there are a variety of mechanisms that can lead to [Ca<sup>2+</sup>]<sub>i</sub> mobilization in epithelial cells, we examined the specificity of the novel compounds for PAR<sub>2</sub>. We redeployed the Ca<sup>2+</sup> mobilization assay in either low expressing PAR<sub>2</sub> HeLa cells and HeLa cells transfected with human PAR<sub>2</sub> (HeLa-PAR<sub>2</sub>) or low expressing kNRK and cells transfected with human PAR<sub>2</sub> (kNRK PAR<sub>2</sub>). We found that 2-furoyl-LIGRLO-NH<sub>2</sub> and the novel compounds 1 and 2 were able to quickly stimulate increases in [Ca<sup>2+</sup>]<sub>i</sub> in HeLa-PAR<sub>2</sub> cells (not shown) or kNRK-PAR<sub>2</sub> cells (Figure 1). In the absence of PAR<sub>2</sub> overexpression, agonist-induced [Ca<sup>2+</sup>]<sub>i</sub> changes were minimized and representative of background PAR<sub>2</sub> expression in these cell types (Figure 1). From these data we conclude that compounds 1 and 2 represent novel, potent, and selective full agonists at PAR<sub>2</sub>.

**In Vitro Physiological Response Assay.** Novel agonists 1 and 2 with Ca<sup>2+</sup> mobilization assay EC<sub>50</sub> values approaching that determined for 2-furoyl-LIGRLO-NH<sub>2</sub> were evaluated along with 2-furoyl-LIGRLO-NH<sub>2</sub> in an in vitro physiological response assay using the xCELLigence real time cell analyzer (RTCA, Table 1).<sup>14</sup> The RTCA records changes in impedance (reported as a cell index) over a prolonged time course in a noninvasive system. These readings represent a physiological output that reflects the combined cellular effects of multiple signaling pathways such as those activated by PAR<sub>2</sub>.<sup>1,4</sup> Each agonist was applied to the cells over an appropriate dose range and cell index was monitored every 15 s for 2 h. We found that agonist activity was similar among the three compounds, with 2-furoyl-LIGRLO-NH<sub>2</sub> and compound 1 displaying nearly identical RTCA EC<sub>50</sub> values and compound 2 displaying less potent activity (Figure 2).

## DISCUSSION

To date, there has not been a comprehensive SAR study on N-terminal modifications of short pentapeptide sequences (e.g., X-LIGRL-NH<sub>2</sub>) built as agonists to PAR<sub>2</sub>. Therefore, we have

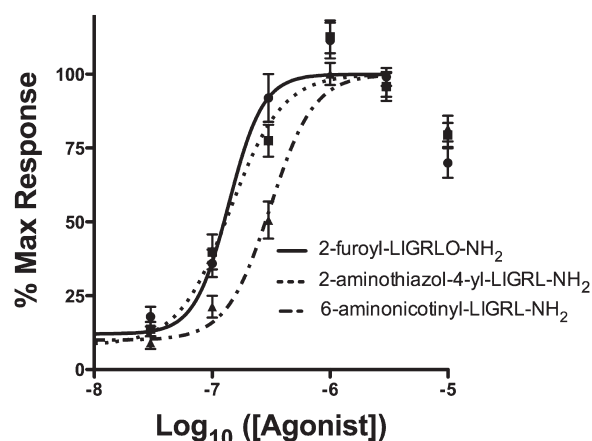
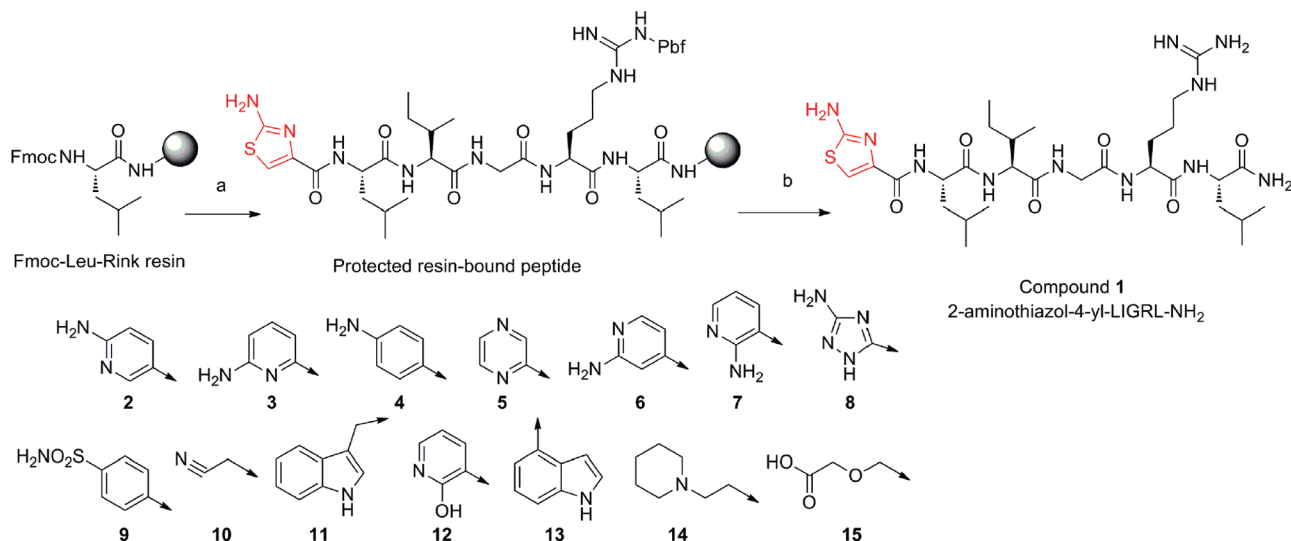


Figure 2. Physiological signaling induced by novel agonists. Dose response curves were calculated based on area under the curve for 2 h of agonist exposure and calculated from 1/2 log dose steps from 10 μM down to 10 nM for each agonist.

designed and synthesized a set of 15 analogues to investigate these N-terminal modifications and their ability to activate PAR<sub>2</sub> (Scheme 1). The analogues were first evaluated using a Ca<sup>2+</sup> mobilization screen. This initial screen indicated a subset of N-terminal modifications that approached the potency of the furan analogue 2-furoyl-LIGRLO-NH<sub>2</sub> with modifications that have structural similarity to be used in further SAR.

We found that aliphatic modifications such as diglycolyl (15), 1-piperidinethyl (14), and 2-cyanomethyl (10) were ineffective (structures are depicted in Scheme 1). Heteroaromatic substituents also did not guarantee PAR<sub>2</sub> activity as documented for indole derivatives (11 and 13) or 2-hydroxypyridinyl (12). However, a subset of heteroaromatic substituents (5–9) elicited [Ca<sup>2+</sup>]<sub>i</sub> activation at the highest doses tested (100 μM) but failed at doses shown to be effective for highest activity compounds (e.g., 10 or 2.5 μM). In this manner, they were as effective as the native peptide sequence (SLIGRL-NH<sub>2</sub>). The most potent agonists created (1–4) share a common structural feature, nitrogen based heterocycle (thiazole or pyridine) with an amino group orientated in the ortho position to the nitrogen (Table 1). 2-aminothiazol-4-yl (1) induced Ca<sup>2+</sup> mobilization EC<sub>50</sub> (1.77 μM) that was higher but not significantly different from that induced by 2-furoyl-LIGRLO-NH<sub>2</sub> (Ca<sup>2+</sup> EC<sub>50</sub> = 0.84 μM). In contrast, 6-aminonicotinyl (Ca<sup>2+</sup> EC<sub>50</sub> = 2.6 μM) (2) and 6-aminopyridin-2-yl (3) (Ca<sup>2+</sup> EC<sub>50</sub> = 3.5 μM) derivatives

Scheme 1. Solid-Phase Synthesis of Compound 1 and Structures of PAR-2 Agonists<sup>a</sup>

<sup>a</sup> (a) (i) Fmoc/<sup>t</sup>Bu synthetic strategy; (ii) 10% piperidine in DMF, 2 + 20 minutes; (iii) HBTU coupling of 2-aminothiazole-4-carboxylic acid; (b) (i) 91% TFA, 3% thioanisole, 3% 1,2-ethanedithiol, 3% water, 4 h; (ii) ether extraction; (iii) HPLC and SEC purifications.

induced Ca<sup>2+</sup> mobilization EC<sub>50</sub> values that were significantly higher than that observed for 2-furoyl-LIGRLO-NH<sub>2</sub>. In 4-aminophenyl (4), the nitrogen atom was removed from the aromatic ring of the nicotinyl residue and the Ca<sup>2+</sup> mobilization EC<sub>50</sub> dropped to 6.5 μM. Other isomers of aminonicotinic acid analogues such as 6-aminopyridin-4-yl (6) and 6-aminopyridin-5-yl (7) or 3-aminotriazine (8) were ineffective at 2.5 μM. From this short peptapeptide SAR we conclude that both the amino group and the aromatic nitrogen contributed to the PAR<sub>2</sub> Ca<sup>2+</sup> signaling agonistic activity.

Because PAR<sub>2</sub> activation can lead to downstream signaling pathways in addition to Ca<sup>2+</sup> signaling, we evaluated the most potent PAR<sub>2</sub> agonists on 16HBE14o- cells using RTCA, an *in vitro* physiological assay. This high-throughput assay detects changes in cell membrane interaction with a tissue culture surface by continually measuring impedance across the tissue culture surface.<sup>14</sup> We selected the two high potency novel agonists (1 and 2) and compared them to the most potent PAR<sub>2</sub> agonist described to date, 2-furoyl-LIGRLO-NH<sub>2</sub>. Both novel agonists (1 and 2) stimulated an increase in cell index in a dose-dependent manner and reached their peak responses within 30 min (not shown). Each compound induced the greatest increase in cell index at a dose of 3 μM, which is approximately 1/10 the concentration required for a maximum response to the native ligand SLIGRL-NH<sub>2</sub> (not shown). Physiological signaling outputs induced by novel agonists (1 and 2) and 2-furoyl-LIGRLO-NH<sub>2</sub> are plotted as dose response curves in Figure 2. The calculated physiological EC<sub>50</sub> values are summarized in Table 1. The physiological EC<sub>50</sub> of the novel agonist 1 was 142 nM, nearly identical to that of 2-furoyl-LIGRLO-NH<sub>2</sub> (138 nM). A significantly higher physiological EC<sub>50</sub> (311 nM) was determined for compound 2. Both agonists (1 and 2) achieved equal E<sub>max</sub> values equivalent to that of the 2-furoyl-LIGRLO-NH<sub>2</sub>,<sup>6</sup> indicating that these novel ligands are full agonists at PAR<sub>2</sub>. This RTCA analysis demonstrates potent activation of model epithelial cells by known and novel PAR<sub>2</sub> agonists and presents a high-throughput *in vitro* physiological assay that allows better comparison of full activity

of PAR<sub>2</sub> agonists than traditional single pathway analyses (e.g., Ca<sup>2+</sup> mobilization).

## EXPERIMENTAL SECTION

**Synthesis.** Peptidomimetics were prepared as previously published by solid-phase synthesis as summarized in Scheme 1 on Rink amide TentaGel resin (0.23 mmol/g) using Fmoc/<sup>t</sup>Bu synthetic strategy and standard DIC and HBTU or HCTU activations.<sup>12c,15</sup> The synthesis was performed in fritted syringes using a Domino manual synthesizer obtained from Torviq (Niles, MI). N-Terminal heterocyclic acids were obtained from Sigma-Aldrich or TCI and coupled using HBTU activation. For compound 4, the Fmoc-protected version (Fmoc-4-aminobenzoic acid) was used and otherwise was acid coupled as purchased. All compounds were fully deprotected and cleaved from the resin by treatment with 91% TFA (3% water, 3% EDT, and 3% TA). After ether extraction of scavengers, compounds were purified by HPLC and/or size-exclusion chromatography (Sephadex G-25, 0.1 M acetic acid) to >95% purity. All compounds were analyzed for purity by analytical HPLC and MS by ESI or MALDI-TOF.

**Ca<sup>2+</sup> Mobilization Assay.** Model epithelial cells (16HBE14o-, HeLa, kNRK) were grown on matrix coated coverslips for 5–7 days with appropriate growth and selection medium. Cells were loaded with the Ca<sup>2+</sup> sensitive dye fura-2 and evaluated for intracellular calcium concentration ([Ca<sup>2+</sup>]<sub>i</sub>) over 3 min using digital imaging microscopy.<sup>13,16</sup> For calculation of Ca<sup>2+</sup> mobilization EC<sub>50</sub>, response was quantified by the percent of cells responding in the field of view with an increase of [Ca<sup>2+</sup>]<sub>i</sub> of ≥ 200 nM. Compounds were initially tested at 100 μM and down to 250 nM, as appropriate (Table 1, Supporting Information Table S2). To demonstrate specificity, the average [Ca<sup>2+</sup>]<sub>i</sub> among all cells (±SEM) in the field of view was calculated over time with [Ca<sup>2+</sup>]<sub>i</sub> measured every 0.6 s (Figure 1).

**In Vitro Physiological Response Assay.** 16HBE14o- cells were plated onto 96-well E-plates (Roche) and grown in fully supplemented growth medium to 95% confluence overnight at 37 °C, 5% CO<sub>2</sub>, and monitored for proliferation using the xCELLigence real time cell analyzer (RTCA; Roche Diagnostics).<sup>14a</sup> Prior to the experiment, well cultures were washed and replaced with 100 μL of modified Hank's balanced saline solution (HBSS) prewarmed to 37 °C and allowed to

come to room temperature (30–45 min). Each well was supplemented with 100  $\mu\text{L}$  of HBSS containing appropriate agonists to measure seven concentrations for three agonists in quadruplicate. Additional wells (eight) were used for HBSS controls (0 mM agonists). Concentrations were from 10  $\mu\text{M}$  to 10 nM in  $1/2$  log steps. Relative impedance in each well was monitored every 15 s over 2 h. For evaluation purposes, relative impedance at any given time is expressed as a “cell index.” Cell index is defined as  $(Z_i - Z_0)/(15 \Omega)$ , where  $Z_i$  is impedance at a given time point during the experiment and  $Z_0$  is impedance before the addition of the agonist. Average cell index for each agonist/dose ( $n = 4$ ) was graphed over time. Physiological  $\text{EC}_{50}$  values were calculated from the area under the curve values.

## ■ ASSOCIATED CONTENT

**S Supporting Information.** Solid phase synthesis, purification and characterization procedures, spectral and HPLC data,  $\text{Ca}^{2+}$  mobilization, and in vitro physiological assays. This material is available free of charge via the Internet at <http://pubs.acs.org>.

## ■ AUTHOR INFORMATION

### Corresponding Author

\*Phone: (520) 626-4179. Fax: (520) 626-4824. E-mail: [vagner@email.arizona.edu](mailto:vagner@email.arizona.edu).

## ■ ACKNOWLEDGMENT

The authors thank the Department of Chemistry, University of Arizona, and more specifically Arpad Somogy for mass spectrometry results. The authors also thank Renata Patek and Zhenyu Zhang for technical assistance, Daniel X. Sherwood for his program that allowed for quick quantification of  $\text{Ca}^{2+}$  data, and Cara L. Sherwood for her help in the laboratory in getting this work going. This work is part of a multiprincipal investigator collaboration between J.V., T.J.P., and S.B. This work was supported in part by the following grants: NIEHS Superfund Research Grant ES 04940 (S.B.), SRC Project 425.024 (S.B.), NIH Grant R01NS065926 (T.J.P.), Technology and Research Initiative Fund from Arizona State Proposition 301 (J.V.), and NIH Training Grant T32-HL007249 (A.N.F.). S.M.S. is a UA UBRP scholar (Grant HHMI 52005889).

## ■ ABBREVIATIONS USED

Aloc, allyloxycarbonyl; Boc, *tert*-butyloxycarbonyl; BB, bromophenol blue;  $\text{CH}_3\text{CN}$ , acetonitrile; DCM, dichloromethane; DI, deionized; DIPEA, diisopropylethylamine; DMF, *N,N*-dimethylformamide; DIC, diisopropylcarbodiimide; DMEM, Dulbecco's modified Eagle medium; Fmoc, fluorenylmethoxycarbonyl; FT-ICR, Fourier Transform ion cyclotron resonance; ESI-MS, electrospray ionization mass spectrometry; EDT, 1,2-ethanedithiol;  $\text{Et}_2\text{O}$ , diethyl ether; HBSS, Hank's balanced saline solution buffered with 25 mM HEPES; HCTU, *O*-[1*H*-(6-chlorobenzotriazol-1-yl)(dimethylamino)ethylene]uranium hexafluorophosphate *N*-oxide; HEPES, 4-(2-hydroxyethyl)-1-piperazineethanesulfonic acid; HOBt, *N*-hydroxybenzotriazole; HOCT, 6-chloro-1-hydroxybenzotriazole; GPCR, G-protein-coupled receptor; MALDI-TOF, matrix assisted laser desorption ionization time of flight;  $\text{PAR}_2$ , protease-activated receptor type 2; Pbf, 2,2,4,6,7-pentamethyl-dihydrobenzofuran-5-sulfonyl; SPPS, solid-phase peptide synthesis; RP-HPLC, reverse-phase high performance liquid chromatography; RCTA, xCELLigence real-time cell analyzer; TA,

thioanisole; THF, tetrahydrofuran; TIS, triisopropylsilane; trifluoroacetic acid; TFA, trifluoroacetic acid

## ■ ADDITIONAL NOTE

Abbreviations used for amino acids and designation of peptides follow the rules of the IUPAC-IUB Commission of Biochemical Nomenclature in *J. Biol. Chem.* **1972**, *247*, 977–983.

## ■ REFERENCES

- (1) (a) Ossovskaya, V. S.; Bunnett, N. W. Protease-activated receptors: contribution to physiology and disease. *Physiol. Rev.* **2004**, *84* (2), 579–621. (b) Ramachandran, R.; Hollenberg, M. D. Proteinases and signalling: pathophysiological and therapeutic implications via PARs and more. *Br. J. Pharmacol.* **2008**, *153* (Suppl. 1), S263–S282.
- (2) (a) Rattenholl, A.; Steinhoff, M. Proteinase-activated receptor-2 in the skin: receptor expression, activation and function during health and disease. *Drug News Perspect.* **2008**, *21* (7), 369–381. (b) Soreide, K. Proteinase-activated receptor 2 (PAR-2) in gastrointestinal and pancreatic pathophysiology, inflammation and neoplasia. *Scand. J. Gastroenterol.* **2008**, *43* (8), 902–909. (c) Bueno, L. Protease activated receptor 2: a new target for IBS treatment. *Eur. Rev. Med. Pharmacol. Sci.* **2008**, *12* (Suppl. 1), 95–102. (d) Mackie, E. J.; Loh, L. H.; Sivagurunathan, S.; Uaesoontrachoon, K.; Yoo, H. J.; Wong, D.; Georgy, S. R.; Pagel, C. N. Protease-activated receptors in the musculoskeletal system. *Int. J. Biochem. Cell Biol.* **2008**, *40* (6–7), 1169–1184. (e) Russo, A.; Soh, U. J.; Trejo, J. Proteases display biased agonism at protease-activated receptors: location matters!. *Mol. Interventions* **2009**, *9* (2), 87–96.
- (3) Vergnolle, N. Protease-activated receptors as drug targets in inflammation and pain. *Pharmacol. Ther.* **2009**, *123* (3), 292–309.
- (4) Soh, U. J.; Dores, M. R.; Chen, B.; Trejo, J. Signal transduction by protease-activated receptors. *Br. J. Pharmacol.* **2010**, *160* (2), 191–203.
- (5) Blackhart, B. D.; Emilsson, K.; Nguyen, D.; Teng, W.; Martelli, A. J.; Nystedt, S.; Sundelin, J.; Scarborough, R. M. Ligand cross-reactivity within the protease-activated receptor family. *J. Biol. Chem.* **1996**, *271* (28), 16466–16471.
- (6) McGuire, J. J.; Saifeddine, M.; Triggle, C. R.; Sun, K.; Hollenberg, M. D. 2-Furoyl-LIGRLO-amide: a potent and selective proteinase-activated receptor 2 agonist. *J. Pharmacol. Exp. Ther.* **2004**, *309* (3), 1124–1131.
- (7) Hollenberg, M. D.; Renaux, B.; Hyun, E.; Houle, S.; Vergnolle, N.; Saifeddine, M.; Ramachandran, R. Derivatized 2-furoyl-LIGRLO-amide, a versatile and selective probe for proteinase-activated receptor 2: binding and visualization. *J. Pharmacol. Exp. Ther.* **2008**, *326* (2), 453–462.
- (8) (a) Barry, G. D.; Le, G. T.; Fairlie, D. P. Agonists and antagonists of protease activated receptors (PARs). *Curr. Med. Chem.* **2006**, *13* (3), 243–265. (b) Barry, G. D.; Suen, J. Y.; Low, H. B.; Pfeiffer, B.; Flanagan, B.; Halili, M.; Le, G. T.; Fairlie, D. P. A refined agonist pharmacophore for protease activated receptor 2. *Bioorg. Med. Chem. Lett.* **2007**, *17* (20), 5552–5557.
- (9) (a) Kawabata, A.; Saifeddine, M.; Al-Ani, B.; Leblond, L.; Hollenberg, M. D. Evaluation of proteinase-activated receptor-1 (PAR1) agonists and antagonists using a cultured cell receptor desensitization assay: activation of PAR2 by PAR1-targeted ligands. *J. Pharmacol. Exp. Ther.* **1999**, *288* (1), 358–370. (b) Ramachandran, R.; Mihara, K.; Mathur, M.; Rochdi, M. D.; Bouvier, M.; Defea, K.; Hollenberg, M. D. Agonist-biased signaling via proteinase activated receptor-2: differential activation of calcium and mitogen-activated protein kinase pathways. *Mol. Pharmacol.* **2009**, *76* (4), 791–801. (c) Gardell, L. R.; Ma, J. N.; Seitzberg, J. G.; Knapp, A. E.; Schiffer, H. H.; Tabatabaei, A.; Davis, C. N.; Owens, M.; Clemons, B.; Wong, K. K.; Lund, B.; Nash, N. R.; Gao, Y.; Lameh, J.; Schmelzer, K.; Olsson, R.; Burstein, E. S. Identification and characterization of novel small-molecule protease-activated receptor 2 agonists. *J. Pharmacol. Exp. Ther.* **2008**, *327* (3), 799–808.
- (10) Williams, D. P.; Antoine, D. J.; Butler, P. J.; Jones, R.; Randle, L.; Payne, A.; Howard, M.; Gardner, I.; Blagg, J.; Park, B. K. The metabolism and toxicity of furosemide in the Wistar rat and CD-1

mouse: a chemical and biochemical definition of the toxicophore. *J. Pharmacol. Exp. Ther.* **2007**, 322 (3), 1208–1220.

(11) (a) Scarborough, R. M. Protease-activated receptor-2 antagonists and agonists. *Curr. Med. Chem.: Cardiovasc. Hematol. Agents* **2003**, 1 (1), 73–82. (b) Maryanoff, B. E.; Santulli, R. J.; McComsey, D. F.; Hoekstra, W. J.; Hoey, K.; Smith, C. E.; Addo, M.; Darrow, A. L.; Andrade-Gordon, P. Protease-activated receptor-2 (PAR-2): structure–function study of receptor activation by diverse peptides related to tethered-ligand epitopes. *Arch. Biochem. Biophys.* **2001**, 386 (2), 195–204.

(12) (a) Vagner, J.; Handl, H. L.; Gillies, R. J.; Hruby, V. J. Novel targeting strategy based on multimeric ligands for drug delivery and molecular imaging: homooligomers of alpha-MSH. *Bioorg. Med. Chem. Lett.* **2004**, 14 (1), 211–215. (b) Josan, J. S.; Vagner, J.; Handl, H. L.; Sankaranarayanan, R.; Gillies, R. J.; Hruby, V. J. Solid-phase synthesis of heterobivalent ligands targeted to melanocortin and cholecystokinin receptors. *Int. J. Pept. Res. Ther.* **2008**, 14 (4), 293–300. (c) Vagner, J.; Xu, L.; Handl, H. L.; Josan, J. S.; Morse, D. L.; Mash, E. A.; Gillies, R. J.; Hruby, V. J. Heterobivalent ligands crosslink multiple cell-surface receptors: the human melanocortin-4 and delta-opioid receptors. *Angew. Chem., Int. Ed.* **2008**, 47 (9), 1685–1688.

(13) Isakson, B. E.; Olsen, C. E.; Boitano, S. Laminin-332 alters connexin profile, dye coupling and intercellular  $Ca^{2+}$  waves in ciliated tracheal epithelial cells. *Respir. Res.* **2006**, 7, 105–116.

(14) (a) Abassi, Y. A.; Xi, B.; Zhang, W.; Ye, P.; Kirstein, S. L.; Gaylord, M. R.; Feinstein, S. C.; Wang, X.; Xu, X. Kinetic cell-based morphological screening: prediction of mechanism of compound action and off-target effects. *Chem. Biol.* **2009**, 16 (7), 712–723. (b) Xi, B.; Yu, N.; Wang, X.; Xu, X.; Abassi, Y. A. The application of cell-based label-free technology in drug discovery. *Biotechnol. J.* **2008**, 3 (4), 484–95.

(15) (a) Krchnak, V.; Vagner, J.; Lebl, M. Noninvasive continuous monitoring of solid-phase peptide synthesis by acid-base indicator. *Int. J. Pept. Protein Res.* **1988**, 32 (5), 415–416. (b) Krchnak, V.; Vagner, J. Color-monitored solid-phase multiple peptide synthesis under low-pressure continuous-flow conditions. *Pept. Res.* **1990**, 3 (4), 182–193.

(16) Olsen, C. E.; Liguori, A. E.; Zong, Y.; Lantz, R. C.; Burgess, J. L.; Boitano, S. Arsenic upregulates MMP-9 and inhibits wound repair in human airway epithelial cells. *Am. J. Physiol.: Lung Cell. Mol. Physiol.* **2008**, 295 (2), L293–302.